

# Perturbation Calculations on Current and Current Noise for the Two-Impurities Anderson Model

Mami HAMASAKI\*

*Department of Material Science, Graduate School of Science, Osaka City University, Osaka 558-8585*

(Received May 29, 2019)

For the two-impurities Anderson model, current and current noise in nonlinear response are studied in terms of the second order perturbation of the on-site Coulomb interactions  $U$  on the basis of the perturbation theory in the Keldysh formalism. Especially, current noise with respect to the second order perturbation of the Coulomb interaction has never been investigated before. Using the numerical calculations, the current conservation is investigated. As the results for the current noise between the two impurities, while the shot noise is enhanced with  $U$  at small  $U$ , at larger  $U$  beyond a slow peak, the shot noise comes to be suppressed more and more with an increase in  $U$ . It is concluded that this change in the shot noise from the enhancement to the suppression is due to the competition between the effect of the self-energy and the effects of the vertex and others.

KEYWORDS: current noise, shot noise, nonequilibrium Green's function, Keldysh formalism, perturbation theory, vertex, self-energy,

## §1. Introduction

Recently, current and current noise in mesoscopic systems have become subjects of extensive researches. The well-known Landauer formula expresses current in terms of the transmission probability through a noninteracting region connected to reservoirs.<sup>1)</sup> However, it is suggested that the Landauer formula is not valid in the case of inelastic scattering by interaction, and a Landauer-like formula for the single impurity Anderson model was derived by use of symmetrization of the currents entering and leaving the impurity (or the central-region) on the assumption that current is uniform in steady state.<sup>2,3)</sup> It is difficult to make a model satisfy the current conservation in the presence of inelastic scattering. Hershfield *et al.* succeeded in conserving the current in nonlinear response and showing the Kondo resonance, including terms up to the second order perturbation of the Coulomb interaction for the symmetric single impurity Anderson model.<sup>4)</sup> Beside this, for the single impurity Anderson model or a quantum dot, there are some cases of conserving current

---

\* E-mail address: hamasaki@sci.osaka-cu.ac.jp

in nonlinear response by use of an approximation for the second order self-energies of the Coulomb interaction.<sup>5,6)</sup>

Current noise is caused by the time-dependent fluctuation of current. In current noise, shot noise and thermal noise are included. In a ballistic system, the quantum effects on shot noise appear clearly. The Khlus-Lesovik formula expresses current noise in terms of the transmission probability through a ballistic noninteracting region;<sup>7,8)</sup> this formula has been confirmed by many experiments.<sup>9,10)</sup> However, the Khlus-Lesovik formula is not valid in case of inelastic scattering by interaction.

The purpose of the present work is to study the current and the current noise in nonlinear response through a ballistic interacting region (*e.g.* a ballistic sample or a quantum wire), in terms of the second order perturbation of the Coulomb interaction. Especially, current noise with respect to the second order perturbation of the Coulomb interaction has never been investigated before. To this end, the current and the current noise are investigated with respect to the second order perturbation of the on-site Coulomb interactions  $U$  on the basis of the perturbation theory in the Keldysh formalism. Generally, current and current noise are expressed between each two sites in the Keldysh formalism<sup>2,3,11,12)</sup> ( excepting the case of only elastic scattering<sup>11,12)</sup> ). Hence, for the single impurity Anderson model, since only the currents and the current noises entering and leaving the impurity can be defined,<sup>2,3)</sup> the current and the current noise flowing through a ballistic interacting region can not be investigated directly. In the present work, for the above reason, the two-impurities Anderson model connected to leads and applied voltage  $eV$  is employed as a minimum model for investigating the current and the current noise flowing through a ballistic interacting region. For the two-impurities Anderson model, the current and the current noise are expressed with respect to the second order perturbation of the on-site Coulomb interactions in the Keldysh formalism. ( In the case of only elastic scattering, these expressions for the current and the current noise are equivalent to the Landauer formula and the Khlus-Lesovik formula, respectively. ) For these expressions, the new full Green's functions are derived from the Dyson equations in the Keldysh formalism. Further, for these full Green's functions, the second order self-energies are derived using the perturbation expansion in the Keldysh formalism. In addition to this, the vertex corrections for the current noise between the two impurities are derived from both the autocorrelation function of the current and the correlation function between the currents with opposite spin to each other, using the perturbation expansion in the Keldysh formalism. For current noise, vertex corrections with respect to the second order perturbation of the Coulomb interaction have never been derived before.

Using the numerical calculations, the current conservation is investigated in the case of low temperatures,  $k_B T < \sim eV$  and high temperatures,  $k_B T > \sim eV$ . As the results for the current noise between the two impurities, while the shot noise is enhanced with  $U$  at small  $U$ , at larger  $U$

beyond a slow peak, the shot noise comes to be suppressed more and more with an increase in  $U$ . (As a matter of course, neither suppression nor enhancement with  $U$  of shot noise appears in the result for the shot noise with respect to the Hartree approximation.) Additionally, the result for the current noise at high temperature ( $k_B T > \sim eV$ ) is presented.

## §2. Model and Nonequilibrium Green's Functions

We consider the system in nonequilibrium and stationary state. The present system is described by the two-impurities Anderson model connected to leads. This model consists of two impurities with the on-site Coulomb interaction  $U$  at the center ( $i = 1$  and  $2$ ) and two perfect leads : the left lead ( $-\infty \leq i \leq 0$ ) and the right lead ( $3 \leq i \leq \infty$ ), connected to the impurities by the mixing matrix elements  $v_L$  and  $v_R$ , respectively. The model is illustrated in Fig. 1. The hopping matrix elements between two impurities and on the two leads are  $W$ . The Hamiltonian is given by  $\mathcal{H} = \mathcal{H}_0 + \mathcal{H}_{\text{mix}} + \mathcal{H}_{\text{Coulomb}}$ , where

$$\mathcal{H}_0 = -W \sum_{i \neq 0,2,\sigma} \left( \hat{C}_{i+1\sigma}^\dagger \hat{C}_{i\sigma} + \text{H.c.} \right), \quad (2.1)$$

$$\mathcal{H}_{\text{mix}} = -v_L \sum_{\sigma} \left( \hat{C}_{1\sigma}^\dagger \hat{C}_{0\sigma} + \text{H.c.} \right) - v_R \sum_{\sigma} \left( \hat{C}_{3\sigma}^\dagger \hat{C}_{2\sigma} + \text{H.c.} \right), \quad (2.2)$$

$$\mathcal{H}_{\text{Coulomb}} = U (\hat{n}_{1\uparrow} \hat{n}_{1\downarrow} + \hat{n}_{2\uparrow} \hat{n}_{2\downarrow}). \quad (2.3)$$

Here, the unperturbed Hamiltonian  $\mathcal{H}_0$  describes the isolated two leads and the two impurities disconnected from two leads. The mixing Hamiltonian  $\mathcal{H}_{\text{mix}}$  connects the two impurities to the two leads. Additionally, the on-site Coulomb interactions on the two impurities are described by  $\mathcal{H}_{\text{Coulomb}}$ .  $\sigma$  is index for spin. The chemical potentials in the left and right leads are  $\mu_L$  and  $\mu_R$ , respectively; thereby, the applied voltage is defined by  $eV \equiv \mu_L - \mu_R$ .

Now, four nonequilibrium Green's functions are introduced by<sup>11, 12, 13, 14)</sup>

$$G_{ij}^>(t_1, t_2) \equiv -i < \hat{C}_i(t_1) \hat{C}_j^\dagger(t_2) >, \quad (2.4)$$

$$G_{ij}^<(t_1, t_2) \equiv i < \hat{C}_j^\dagger(t_2) \hat{C}_i(t_1) >, \quad (2.5)$$

$$G_{ij}^r(t_1, t_2) \equiv -i\theta(t_1 - t_2) < \{ \hat{C}_i(t_1), \hat{C}_j^\dagger(t_2) \} >, \quad (2.6)$$

$$G_{ij}^a(t_1, t_2) \equiv i\theta(t_2 - t_1) < \{ \hat{C}_i(t_1), \hat{C}_j^\dagger(t_2) \} >, \quad (2.7)$$

where  $\langle \dots \rangle$  denotes a thermal average in nonequilibrium and curly brackets denote the anticommutator. Note that the four nonequilibrium Green's functions satisfy the relation in the Keldysh formalism :  $G_{ij}^a - G_{ij}^r = G_{ij}^< - G_{ij}^>$ .

A thermal average in nonequilibrium can be obtained on the basis of the perturbation theory in the Keldysh formalism.<sup>13, 14)</sup> Initially at  $t = -\infty$ , it is assumed that the two impurities are disconnected from two leads; thereby, the two impurities and the two leads are in their respective thermal equilibrium. Then the mixing matrix elements are turned on adiabatically. After that, the

time evolution of the density matrix is formulated with respect to the time loop which starts and ends at  $t = -\infty$  as illustrated in Fig. 2.

### §3. Current and Current Noise

For the Hamiltonian described in the previous section, the current operator can be written by

$$\hat{J}_\sigma(i-1, i; t) = \frac{ieW}{\hbar} \left[ \hat{C}_{i\sigma}^\dagger(t) \hat{C}_{i-1\sigma}(t) - \hat{C}_{i-1\sigma}^\dagger(t) \hat{C}_{i\sigma}(t) \right]. \quad (3.1)$$

Accordingly, the average current flowing between two sites is expressed by<sup>2,3,11,12)</sup>

$$\langle 2\hat{J}_\sigma(i-1, i) \rangle = \frac{2eW}{\hbar} \int dE \left[ G_{i-1,i\sigma}^<(E) - G_{i,i-1\sigma}^<(E) \right]. \quad (3.2)$$

The current noise at zero-frequency is defined by

$$S_{\sigma\sigma'} \equiv 2 \int dt \left[ \langle \hat{J}_\sigma(t) \hat{J}_{\sigma'}(0) \rangle - \langle \hat{J}_\sigma \rangle \langle \hat{J}_{\sigma'} \rangle \right]. \quad (3.3)$$

By substituting eq.(3.1) into eq.(3.3), we can formulate the current noise between two sites at zero-frequency. If the vertex is ignored, an expression for the current noise is formed from the autocorrelation function of the current:

$$\begin{aligned} 2S_{\sigma\sigma}^0(i-1, i) = -2 \left( \frac{2e^2W^2}{\hbar} \right) \int dE & \left[ G_{i,i-1\sigma}^<(E) G_{i,i-1\sigma}^>(E) \right. \\ & - G_{i-1,i-1\sigma}^<(E) G_{i,i\sigma}^>(E) \\ & - G_{i,i\sigma}^<(E) G_{i-1,i-1\sigma}^>(E) \\ & \left. + G_{i-1,i\sigma}^<(E) G_{i-1,i\sigma}^>(E) \right]; \end{aligned} \quad (3.4)$$

the diagram is illustrated in Fig. 3. In eqs.(3.2) and (3.4), the factor of 2 is for spin. In the case of only elastic scattering, *e.g.*, the Hartree approximation, eq.(3.2) is equivalent to the Landauer formula,<sup>1)</sup> and eq.(3.4) is equivalent to the Khlus-Lesovik formula for one channel at zero-frequency.<sup>7,8)</sup>

Next, in addition to the current noise defined by eq.(3.4) ( the self-energy term ), the vertex corrections are derived for the current noise between the two impurities. Again, we substitute eq.(3.1) into eq.(3.3) and execute the diagrammatical expansion with respect to the second order perturbation of the on-site Coulomb interactions in the Keldysh formalism, and consequently, we can obtain three kinds of vertex corrections for the current noise between the two impurities. Each vertex correction is composed of sixty-four terms. Three kinds of diagrams for these vertex corrections are illustrated in Figs. 4(a), 4(b) and 4(c). Here, the solid line denotes the full Green's function ( the interacting Green's function ), presented in the next section, and the thin solid line denotes the noninteracting Green's function, which includes the mixing of the two leads with the two impurities in the absence of the Coulomb interactions. A kind of vertex correction of them,  $\delta S_a$ , illustrated in Fig. 4(a), is derived from the autocorrelation function of the current. Two other kinds of vertex corrections,  $\delta S_b$  and  $\delta S_c$ , illustrated in Figs. 4(b) and 4(c) respectively, are derived

from the correlation function between the currents whose spin is opposite to each other. If the indices for spins are omitted, then the vertex correction  $\delta S_a$  illustrated in Fig. 4(a) and  $\delta S_b$  in Fig. 4(b) are equivalent.

#### §4. Full Green's Functions

To express the current and the current noise mentioned in the previous section, the full Green's functions are presented. Solving the Dyson equations in the Keldysh formalism, we can get the full Green's functions for the two-impurities Anderson model. The retarded Green's functions are expressed by

$$G_{11}^r = \frac{1}{E - \Sigma_{11U}^r - v_L^2 F_L^r - (W + \Sigma_{12U}^r)(W + \Sigma_{21U}^r)G_{22R}^r}, \quad (4.1)$$

$$G_{22}^r = \frac{1}{E - \Sigma_{22U}^r - v_R^2 F_R^r - (W + \Sigma_{12U}^r)(W + \Sigma_{21U}^r)G_{11L}^r}, \quad (4.2)$$

$$G_{12}^r = G_{11}^r (W + \Sigma_{12U}^r) G_{22R}^r = G_{11L}^r (W + \Sigma_{12U}^r) G_{22}^r, \quad (4.3)$$

$$G_{21}^r = G_{22}^r (W + \Sigma_{21U}^r) G_{11L}^r = G_{22R}^r (W + \Sigma_{21U}^r) G_{11}^r. \quad (4.4)$$

Here

$$G_{11L}^r = \frac{1}{E - \Sigma_{11U}^r - v_L^2 F_L^r}, \quad (4.5)$$

$$G_{22R}^r = \frac{1}{E - \Sigma_{22U}^r - v_R^2 F_R^r}, \quad (4.6)$$

$$G_{11R}^r = \frac{1}{E - \Sigma_{11U}^r - (W + \Sigma_{12U}^r)(W + \Sigma_{21U}^r)G_{22R}^r}, \quad (4.7)$$

$$G_{22L}^r = \frac{1}{E - \Sigma_{22U}^r - (W + \Sigma_{12U}^r)(W + \Sigma_{21U}^r)G_{11L}^r}. \quad (4.8)$$

Further, using these retarded Green's functions, the lesser Green's functions are written by

$$G_{11}^< = G_{11}^r \left[ i f_L \Gamma_L - \Sigma_{11U}^< + (W + \Sigma_{12U}^r) G_{22R}^< (W + \Sigma_{21U}^a) \right. \\ \left. - (W + \Sigma_{12U}^r) G_{22R}^r \Sigma_{21U}^< - \Sigma_{12U}^< G_{22R}^a (W + \Sigma_{21U}^a) \right] G_{11}^a, \quad (4.9)$$

$$G_{22}^< = G_{22}^r \left[ i f_R \Gamma_R - \Sigma_{22U}^< + (W + \Sigma_{21U}^r) G_{11L}^< (W + \Sigma_{12U}^a) \right. \\ \left. - (W + \Sigma_{21U}^r) G_{11L}^r \Sigma_{12U}^< - \Sigma_{21U}^< G_{11L}^a (W + \Sigma_{12U}^a) \right] G_{22}^a, \quad (4.10)$$

$$G_{12}^< = G_{11}^r (W + \Sigma_{12U}^r) G_{22R}^< + G_{11}^< (W + \Sigma_{12U}^a) G_{22R}^a - G_{11}^r \Sigma_{12U}^< G_{22R}^a \\ = G_{11L}^r (W + \Sigma_{12U}^r) G_{22}^< + G_{11L}^< (W + \Sigma_{12U}^a) G_{22}^a - G_{11L}^r \Sigma_{12U}^< G_{22}^a, \quad (4.11)$$

$$G_{21}^< = G_{22}^r (W + \Sigma_{21U}^r) G_{11L}^< + G_{22}^< (W + \Sigma_{21U}^a) G_{11L}^a - G_{22}^r \Sigma_{21U}^< G_{11L}^a \\ = G_{22R}^r (W + \Sigma_{21U}^r) G_{11}^< + G_{22R}^< (W + \Sigma_{21U}^a) G_{11}^a - G_{22R}^r \Sigma_{21U}^< G_{11}^a. \quad (4.12)$$

Here

$$G_{11L}^< = G_{11L}^r \left[ i f_L \Gamma_L - \Sigma_{11U}^< \right] G_{11L}^a, \quad (4.13)$$

$$G_{22R}^< = G_{22R}^r \left[ i f_R \Gamma_R - \Sigma_{22U}^< \right] G_{22R}^a, \quad (4.14)$$

$$\begin{aligned} G_{11R}^< = G_{11R}^r \left[ -\Sigma_{11U}^< + (W + \Sigma_{12U}^r) G_{22R}^< (W + \Sigma_{21U}^a) \right. \\ \left. - (W + \Sigma_{12U}^r) G_{22R}^r \Sigma_{21U}^< - \Sigma_{12U}^< G_{22R}^a (W + \Sigma_{21U}^a) \right] G_{11R}^a, \end{aligned} \quad (4.15)$$

$$\begin{aligned} G_{22L}^< = G_{22L}^r \left[ -\Sigma_{22U}^< + (W + \Sigma_{21U}^r) G_{11L}^< (W + \Sigma_{12U}^a) \right. \\ \left. - (W + \Sigma_{21U}^r) G_{11L}^r \Sigma_{12U}^< - \Sigma_{21U}^< G_{11L}^a (W + \Sigma_{12U}^a) \right] G_{22L}^a. \end{aligned} \quad (4.16)$$

In addition, the full Green's functions for the outside sites of the two impurities can be obtained by

$$G_{00}^r = \frac{1}{E - v_L^2 G_{11R}^r - W^2 F_L^r}, \quad (4.17)$$

$$G_{33}^r = \frac{1}{E - v_R^2 G_{22L}^r - W^2 F_R^r}, \quad (4.18)$$

$$G_{00}^< = G_{00}^r \left[ v_L^2 G_{11R}^< + i f_L \Gamma_L W^2 / v_L^2 \right] G_{00}^a, \quad (4.19)$$

$$G_{33}^< = G_{33}^r \left[ v_R^2 G_{22L}^< + i f_R \Gamma_R W^2 / v_R^2 \right] G_{33}^a, \quad (4.20)$$

$$G_{01}^< = v_L F_L^r G_{11}^< + i f_L \Gamma_L G_{11}^a / v_L, \quad (4.21)$$

$$G_{10}^< = v_L F_L^a G_{11}^< + i f_L \Gamma_L G_{11}^r / v_L, \quad (4.22)$$

$$G_{32}^< = v_R F_R^r G_{22}^< + i f_R \Gamma_R G_{22}^a / v_R, \quad (4.23)$$

$$G_{23}^< = v_R F_R^a G_{22}^< + i f_R \Gamma_R G_{22}^r / v_R. \quad (4.24)$$

Note that all Green's functions depend on energy  $E$ . Here,  $f_L$  and  $f_R$  are the Fermi distribution functions in the left and right leads, respectively and  $\Sigma$  is self-energy. The coupling functions with the left and right leads are  $\Gamma_L = -2v_L^2 \text{Im}F_L^r$  and  $\Gamma_R = -2v_R^2 \text{Im}F_R^r$ . Here,  $F_L^r$  and  $F_R^r$  are the Green's functions in the isolated left and right leads respectively; these are taken by  $F_L^r(i) = [E - W^2 F_L^r(i-1)]^{-1}$  and  $F_R^r(i) = [E - W^2 F_R^r(i+1)]^{-1}$  from the recursive relations,<sup>11, 12, 15, 16)</sup> and satisfy the following conditions in the isolated leads:<sup>11, 12, 15, 16)</sup>  $F_L^r = F_L^r(i) = F_L^r(i-1)$ ,  $F_R^r = F_R^r(i) = F_R^r(i+1)$ .

Next, for the two-impurities Anderson model, the second order self-energies of the on-site Coulomb interactions can be taken by use of the perturbation expansion in the Keldysh formalism:

$$\begin{aligned} \Sigma_{mn\sigma}^{r(2)}(E) = \Sigma_{nm\sigma}^{a*(2)}(E) \\ = U^2 \int \frac{dE_1}{2\pi} \int \frac{dE_2}{2\pi} \left[ g_{mn\sigma}^r(E_1) g_{mn-\sigma}^>(E_2) g_{nm-\sigma}^<(E_1 + E_2 - E) \right. \\ \left. + g_{mn\sigma}^<(E_1) g_{mn-\sigma}^r(E_2) g_{nm-\sigma}^>(E_1 + E_2 - E) \right. \\ \left. + g_{mn\sigma}^<(E_1) g_{mn-\sigma}^>(E_2) g_{nm-\sigma}^a(E_1 + E_2 - E) \right], \end{aligned} \quad (4.25)$$

$$\Sigma_{mn\sigma}^{<(2)}(E) = -U^2 \int \frac{dE_1}{2\pi} \int \frac{dE_2}{2\pi} g_{mn\sigma}^<(E_1) g_{mn-\sigma}^<(E_2) g_{nm-\sigma}^>(E_1 + E_2 - E), \quad (4.26)$$

$$\Sigma_{mn\sigma}^{>(2)}(E) = -U^2 \int \frac{dE_1}{2\pi} \int \frac{dE_2}{2\pi} g_{mn\sigma}^>(E_1) g_{mn-\sigma}^>(E_2) g_{nm-\sigma}^<(E_1 + E_2 - E), \quad (4.27)$$

$(m, n = 1 \text{ or } 2)$ .

Here,  $g$  is the noninteracting Green's function. Note that these self-energies satisfy the relation in the Keldysh formalism :  $\Sigma_{mn}^{r(2)} - \Sigma_{mn}^{a(2)} = \Sigma_{mn}^{<(2)} - \Sigma_{mn}^{>(2)}$ . The diagram for the second order self-energies is illustrated in Fig. 5. Using the full Green's functions in which these self-energies are inserted, the current and the current noise mentioned in the previous section can be expressed.

## §5. Numerical Results and Discussion

The numerical results for the current and the current noise are presented and discussed. The  $U$  dependence of the current and the current noise is investigated in the symmetric case of  $\Gamma_L = \Gamma_R$  and the electron-hole symmetry:  $\mu_L = -\mu_R = eV/2$ . The numerical calculations are carried out for  $U/W = 0 \sim 5.5$ ,  $eV/W = 0.3$  and  $v_L/W = v_R/W = 0.8$  at temperatures  $k_B T/W = 0.0, 0.1, 0.6$  and 1.0. All energy integrals are done in the range of one-dimensional energy-band.

The current conservation for the two-impurities Anderson model connected to leads is investigated in the case of zero and finite temperatures. The current entering the impurities from the left lead,  $\langle \hat{J}(0,1) \rangle$  and the current leaving the impurities to the right lead,  $\langle \hat{J}(2,3) \rangle$  are equivalent at any temperatures. The  $U$  dependence of the currents is shown in Figs. 6(a), 6(b) and 6(c). As shown in Figs. 6(a) and 6(b), the current flowing between the two impurities,  $\langle \hat{J}(1,2) \rangle$  is not equivalent but approximately equal to  $\langle \hat{J}(0,1) \rangle$  and  $\langle \hat{J}(2,3) \rangle$ ; accordingly, it can be estimated that the current is conserved at low temperatures. At high temperatures,  $k_B T/W = 0.6$  and 1.0, i.e., when the temperature is large in comparison with the applied voltage:  $k_B T \sim eV$ , the current conservation comes to break at larger  $U$  than shown in Fig. 6(c). ( Note that in only elastic scattering, the current is perfectly conserved at any temperatures. ) At any temperatures, the current damps with increasing  $U$ ; it is the effect of the inelastic scattering by the Coulomb interactions. Besides the current is reduced at high temperatures, as shown in Fig. 6(c).

Next, the results for the current noise between the two impurities are presented. Figures 7(a) and 8 show the  $U$  dependence of the current noise taken from the autocorrelation function of the current: the self-energy term  $S^0$ , the vertex correction  $\delta S_a$  and the total current noise  $S = S^0 + \delta S_a$ . The two other vertex corrections, derived from the correlation function between the currents whose spin is opposite to each other, cancel approximately:  $\delta S_b = -\delta S_c$ , so that they do not contribute to the current noise. This result is valid in view of the Ward identities.

Figure 7(a) shows the  $U$  dependence of the shot noise at zero temperature. While the shot noise is enhanced with  $U$  at small  $U$ , at larger  $U$  beyond a slow peak, the shot noise comes to be suppressed more and more with an increase in  $U$ . From Fig. 7(a), it is found that the enhancement with  $U$  of the shot noise at small  $U$  is mainly due to the vertex correction  $\delta S_a$  though that the self-energy term  $S^0$  is also enhanced somewhat at small  $U$ . In contrast, it is concluded that the shot noise is suppressed at larger  $U$  owing to the effect of the self-energy, from the following: if the vertex correction is expressed in terms of only the noninteracting Green's function, the vertex correction never damps at larger  $U$ . Furthermore, the following is deduced: because the effect of

the self-energy on the shot noise is weak at small  $U$ , the self-energy hardly affects the shot noise and the effects of the vertex and others are dominant at small  $U$ ; contrary to this, at larger  $U$ , the effect of the self-energy dominates those of the vertex and others, so that the shot noise is suppressed at larger  $U$ . Thus, it is concluded that the change in the shot noise from the enhancement to the suppression is due to the competition between the effect of the self-energy and the effects of the vertex and others.

Next, the results of the suppression and the enhancement with  $U$  on the shot noise are discussed from a physical point of view. For the enhancement of the shot noise at small  $U$ , it is explained that the transmission probability decreases effectively because of the inelastic scattering by the Coulomb interactions and that the shot noise is enhanced for the lower transmission probability. Further, the result of the suppression on the shot noise at larger  $U$  is discussed. Figure 7(b) shows the  $U$  dependence of the Fano factor. The Fano factor also damps at larger  $U$  beyond a slow peak in Fig. 7(b). From this, it is found that the shot noise damps more rapidly than the current at larger  $U$ . Additionally, only the self-energy term  $S^0$  also damps more rapidly than the current at larger  $U$ . In general, it is known that in the limit of low transmission probability, shot noise reaches the Poisson value,<sup>17)</sup> i.e., shot noise comes to be proportional to the current and the Fano factor comes to be unity. However, from the results, it is inferred that the suppression of the shot noise at larger  $U$  in the present system is not connected with the case of the limit of low transmission probability. For the origin of suppression of shot noise in the presence of the Coulomb interaction, there are two possibilities: the effect of the Coulomb correlation and the effect of the inelastic scattering by the Coulomb interactions. In general, it is thought that the Coulomb repulsion suppresses shot noise because of the Coulomb repulsion preventing electron from bunching.<sup>18,19,20)</sup> In connection with the effect of the inelastic scattering, it was analytically shown that shot noise at low-frequency is suppressed in the presence of energy dissipation.<sup>21)</sup> Although the present system is not directly connected with the energy dissipation, the present system expresses the inelastic process. As discussed earlier, the current damps with increasing  $U$ ; this is the effect of the inelastic scattering by the Coulomb interactions. Thus, it is expected that shot noise generated in nonequilibrium is also affected directly by the inelastic scattering itself. However, neither mechanisms in the effects of the Coulomb correlation nor inelastic scattering on shot noise have yet been made clear sufficiently.

Figure 8 shows the  $U$  dependence of the current noise at  $k_B T/W = 1.0$ . The current noise increases more and more with temperature owing to the thermal noise. ( Note that the scales of the axes in Figs. 7(a) and 8 differ respectively. ) At  $k_B T/W > \sim 0.5$ , the vertex correction  $\delta S_a$  changes to negative (i.e.,  $\delta S_c$  changes to positive). In Fig. 8, it is shown that the self-energy term  $S^0$  is reduced monotonously with an increase in  $U$  and that the vertex correction  $\delta S_a$  also reduces the current noise consistently. It is inferred that thermal noise is dominant at high temperatures, i.e.,  $k_B T > \sim eV$ . Experimentally, thermal noise has been observed to be proportional to the

transmission probability.<sup>10)</sup> Hence, it is concluded that at high temperatures, the current noise is reduced with a effective decrease in the transmission probability owing to the inelastic scattering.

## §6. Conclusions

For the two-impurities Anderson model, current and current noise in nonlinear response are studied in terms of the second order perturbation of the on-site Coulomb interactions on the basis of the perturbation theory in the Keldysh formalism. Especially, current noise with respect to the second order perturbation of the Coulomb interaction has never been investigated before. Using the numerical calculations, the current conservation is investigated in the case of low temperatures,  $k_B T < \sim eV$  and high temperatures,  $k_B T > \sim eV$ . Further, as the results for the current noise between the two impurities, while the shot noise is enhanced with  $U$  at small  $U$ , at larger  $U$  beyond a slow peak, the shot noise comes to be suppressed more and more with an increase in  $U$ . It is concluded that this change in the shot noise from the enhancement to the suppression is due to the competition between the effect of the self-energy and the effects of the vertex and others. Additionally, the current noise is reduced monotonously with increasing  $U$  at high temperature,  $k_B T > \sim eV$ . The vertex correction reduces the current noise because the vertex correction changes to negative at high temperatures.

Furthermore, as future subjects, the author thinks that for shot noise, the terms higher than the second order perturbation of the Coulomb interaction should also be investigated.

---

- [1] R. Landauer : Philos. Mag. **21** (1970) 863.
- [2] Y. Meir and N. S. Wingreen : Phys. Rev. Lett **68** (1992) 2512; A. P. Jauho, N. S. Wingreen and Y. Meir : Phys. Rev. B **50** (1994) 5528.
- [3] A. P. Jauho: cond-mat/0208577.
- [4] S. Hershfield, J. H. Davies and J. W. Wilkins : Phys. Rev. B **46** (1992) 7046.
- [5] R. Fazio and R. Raimondi : Phys. Rev. Lett **80** (1998) 2913.
- [6] D. Matsumoto : J. Phys. Soc. Jpn. **69** (2000) 1449.
- [7] V. A. Khlus : Zh. Eksp. Teor. Fiz. **93** (1987) 2179 ; Sov. Phys. JETP **66** (1987) 1243.
- [8] G. B. Lesovik : Pis'ma Zh. Eksp. Teor. Fiz. **49** (1989) 513 ; JETP Lett. **49** (1989) 593.
- [9] A. Kumar, L. Saminadayar, D. C. Glattli, Y. Jin and B. Etienne : Phys. Rev. Lett. **76** (1996) 2778.
- [10] M. Henny, S. Oberholzer, C. Stunk, T. Heinzel, K. Ensslin, M. Holland and C. Schönenberger : Science **284** (1999) 296.
- [11] S. Nonoyama and A. Oguri : Phys. Rev. B **57** (1998) 8797.
- [12] S. Nonoyama and A. Oguri : J. Phys. Soc. Jpn. **69** (2000) 1145.
- [13] L. V. Keldysh : Zh. Eksp. Teor. Fiz. **47** (1965) 1515 ; Sov. Phys. JETP **20** (1965) 1018.
- [14] C. Caroli, R. Combescot, P. Nozieres and D. Saint-James : J. Phys. C **4** (1971) 916.
- [15] S. Nonoyama, A. Oguri, Y. Asano and S. Maekawa : Phys. Rev. B **50** (1994) 2667.
- [16] S. Nonoyama and A. Oguri : J. Phys. Soc. Jpn. **64** (1995) 3871.
- [17] For a review, see Ya. M. Blanter and M. Büttiker : Phys. Rep. **336** (2000) 1.
- [18] For a review, see R. Landauer : Nature **392** (1998) 658.

- [19] M. Reznikov, M. Heiblum , H. Shtrikman and D. Mahalu : Phys. Rev. Lett. **75** (1995) 3340.
- [20] H. Birk, M. J. M. de Jong and C. Schonenberger: Phys. Rev. Lett. **75** (1995) 1610.
- [21] M. Ueda and A. Shimizu : J. Phys. Soc. Jpn. **62** (1993) 2994.

Fig. 1 The two-impurities Anderson model connected to leads. Two impurities at the center ( $i = 1$  and  $2$ ) and two perfect leads : the left lead ( $-\infty \leq i \leq 0$ ) and the right lead ( $3 \leq i \leq \infty$ ).

Fig. 2 The time loop starts and ends at  $t = -\infty$ .

Fig. 3 The diagram for the current noise derived from the autocorrelation function of the current without respect of vertices.

Fig. 4(a)(b)(c) Three kinds of diagrams for the vertex corrections with respect to the second order perturbation. The solid line and the thin solid line denote the full Green's function and the noninteracting Green's function, respectively.

Fig. 5 The diagram for the second order self-energies.

Fig. 6 The  $U$  dependence of the currents: the current flowing between the two impurities  $\langle \hat{J}(1,2) \rangle$  ( solid line ), and the current entering the impurities  $\langle \hat{J}(0,1) \rangle$  and the current leaving the impurities  $\langle \hat{J}(2,3) \rangle$  ( dashed line ), at temperatures (a)  $k_B T/W = 0.0$ , (b)  $k_B T/W = 0.1$  and (c)  $k_B T/W = 0.0, 0.6$  and  $1.0$ .

Fig. 7 (a) The  $U$  dependence of the shot noise between the two impurities at zero temperature: the self-energy term  $S^0$  ( dashed line ), the vertex correction  $\delta S_a$  ( dotted line ) and the total shot noise  $S$  ( solid line ). (b) The  $U$  dependence of the Fano factor at zero temperature.

Fig. 8 The  $U$  dependence of the current noise between the two impurities at  $k_B T/W = 1.0$ : the self-energy term  $S^0$  ( dashed line ), the vertex correction  $\delta S_a$  ( dotted line ) and the total current noise  $S$  ( solid line ).

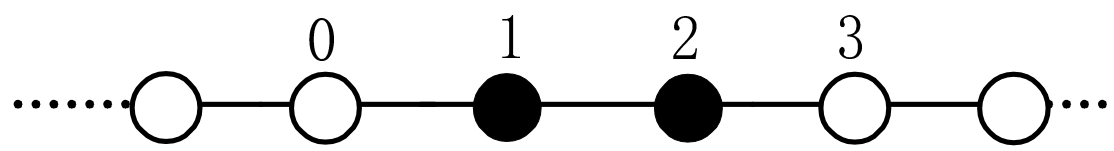


Fig.1      Hamasaki

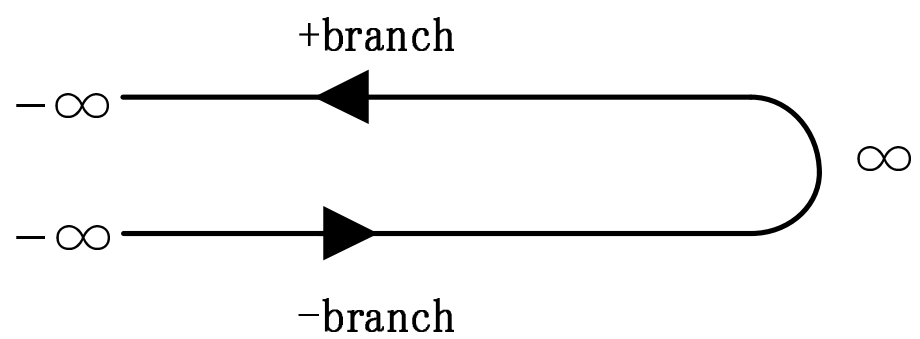


Fig.2      Hamasaki

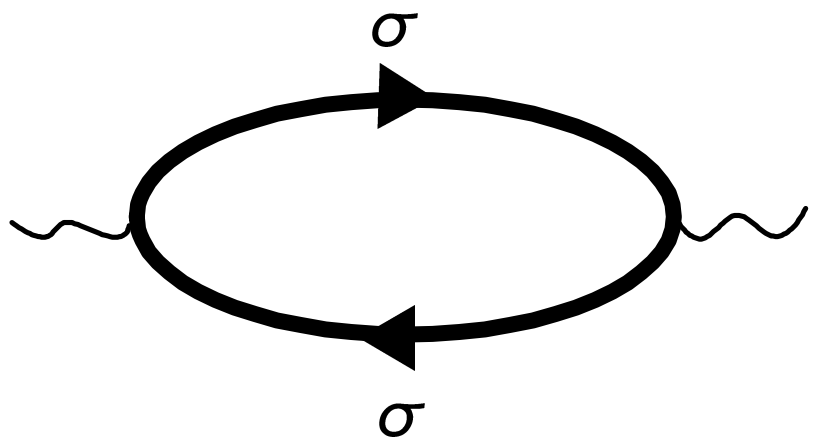


Fig.3   Hamasaki

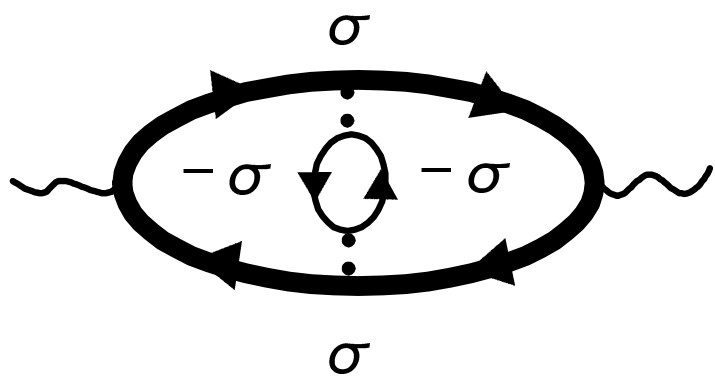


Fig.4(a)      Hamasaki

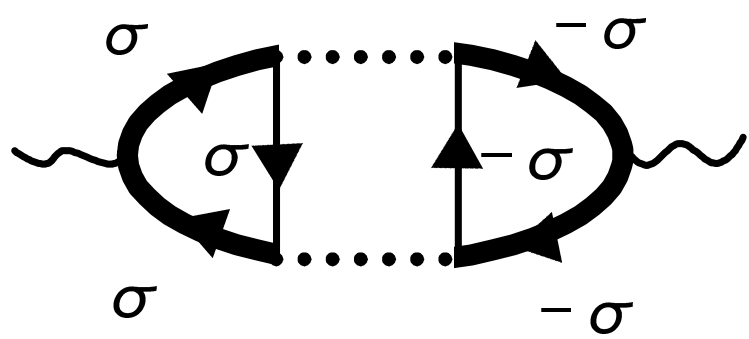


Fig.4(b)      Hamasaki

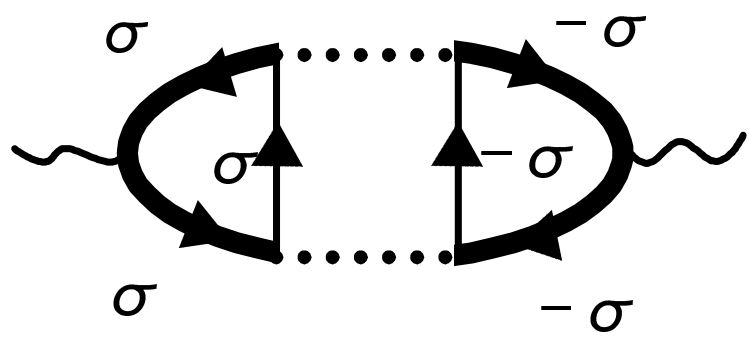


Fig.4(c)      Hamasaki

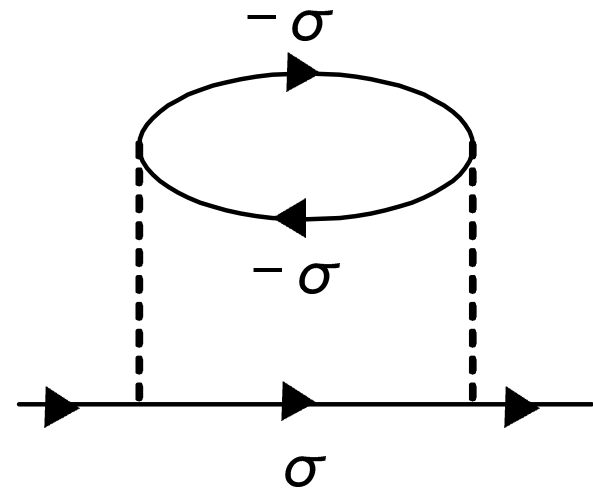


Fig.5 Hamasaki

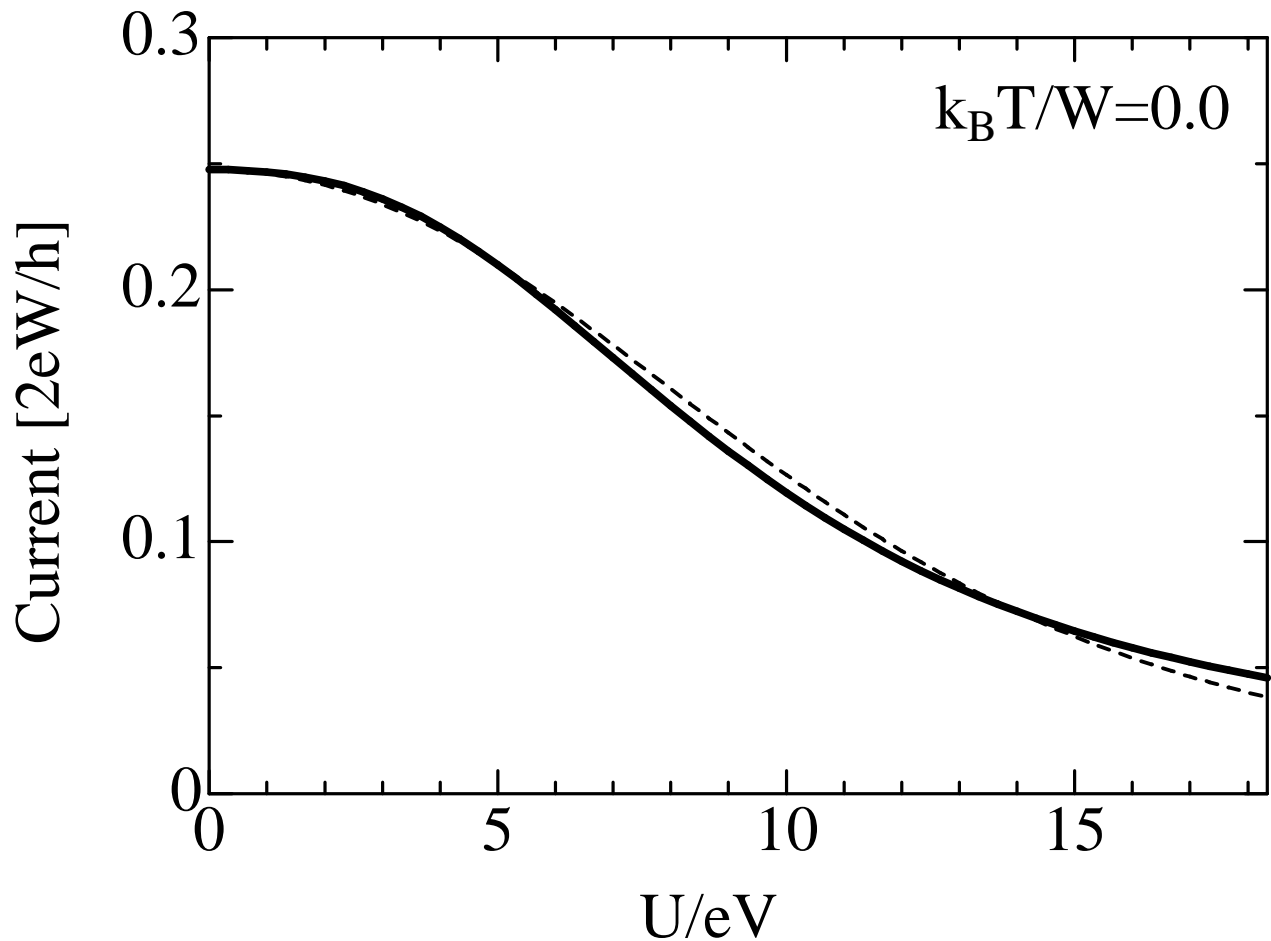


Fig.6(a)    Hamasaki

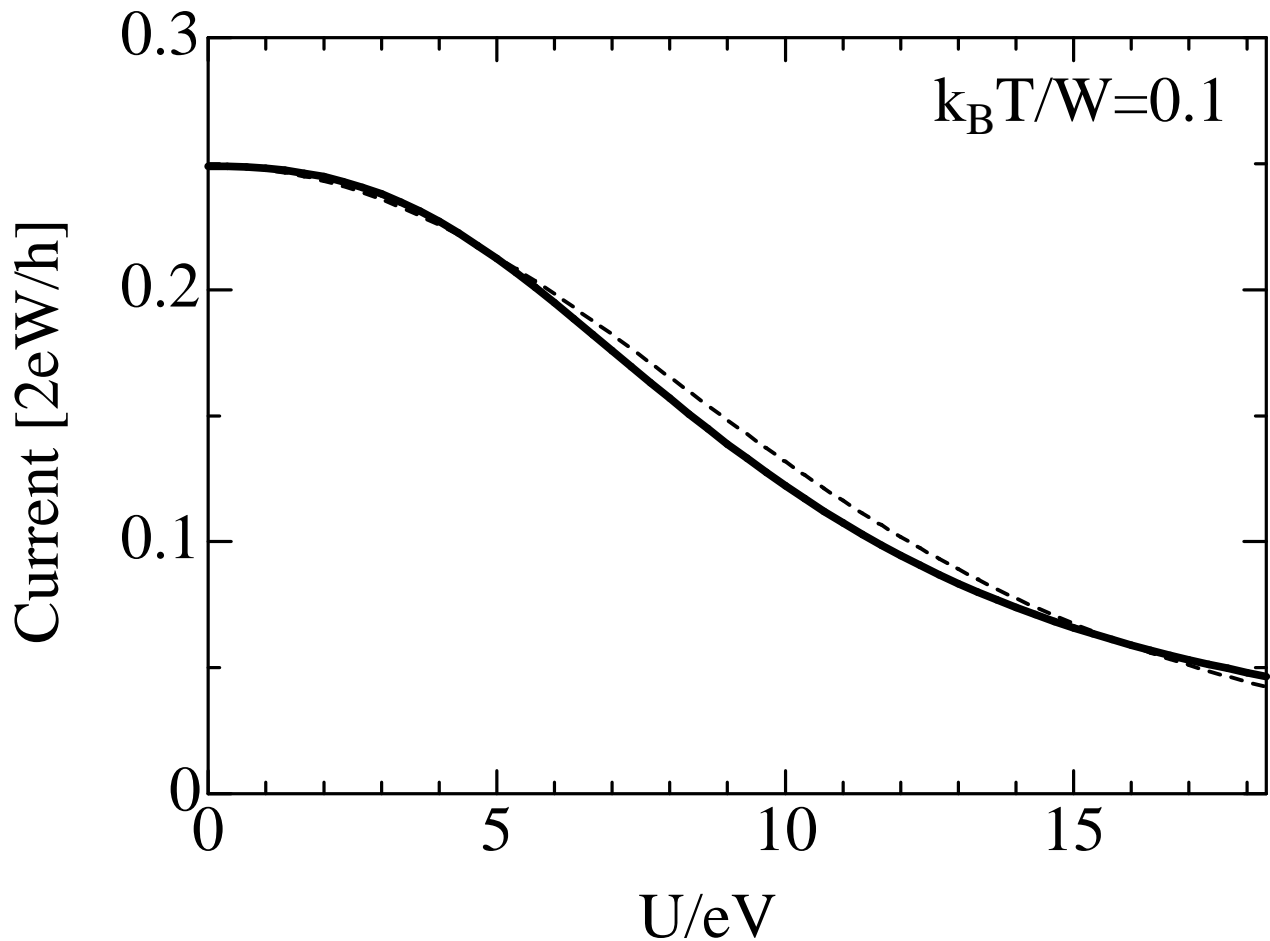


Fig.6(b)    Hamasaki

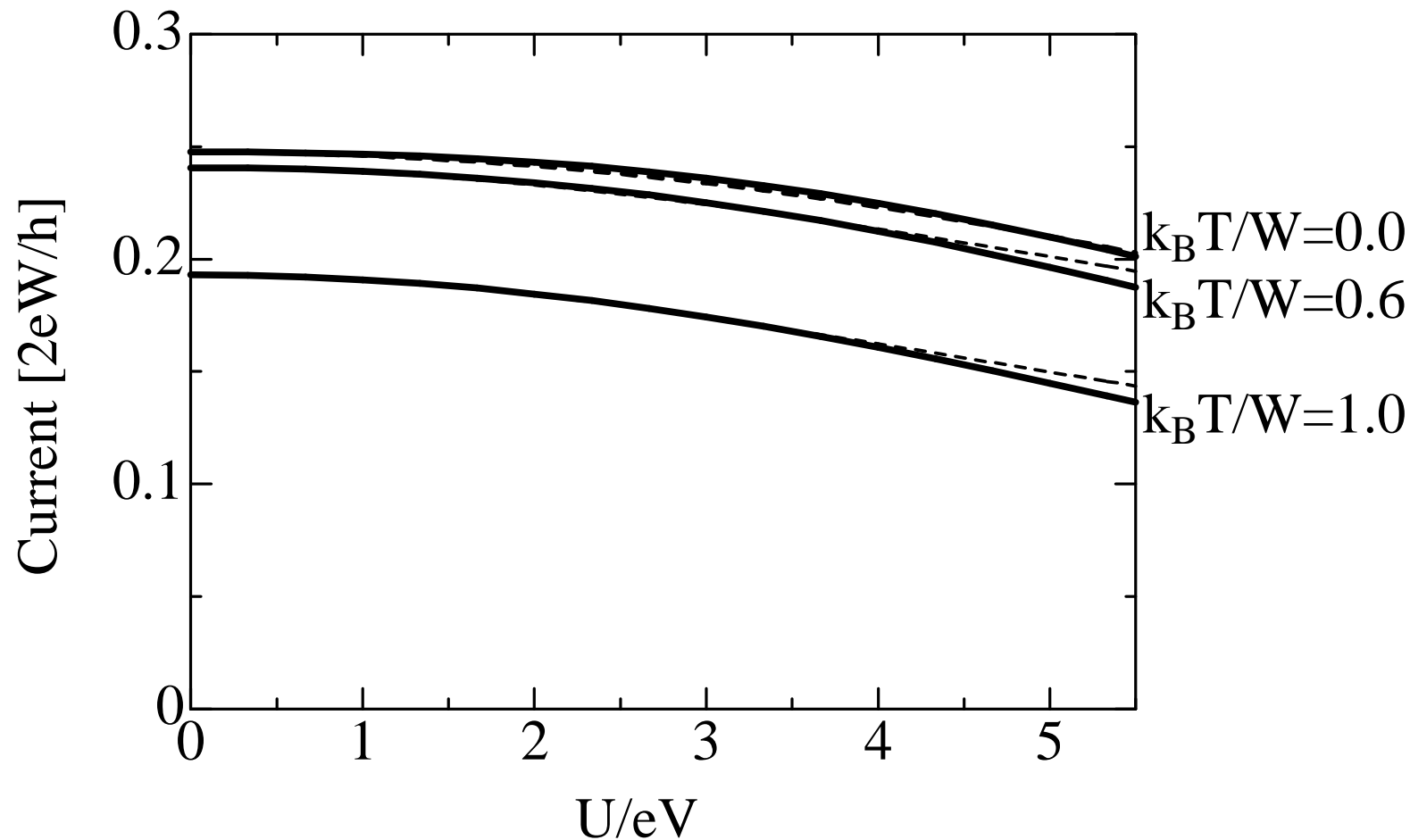


Fig.6(c) Hamasaki

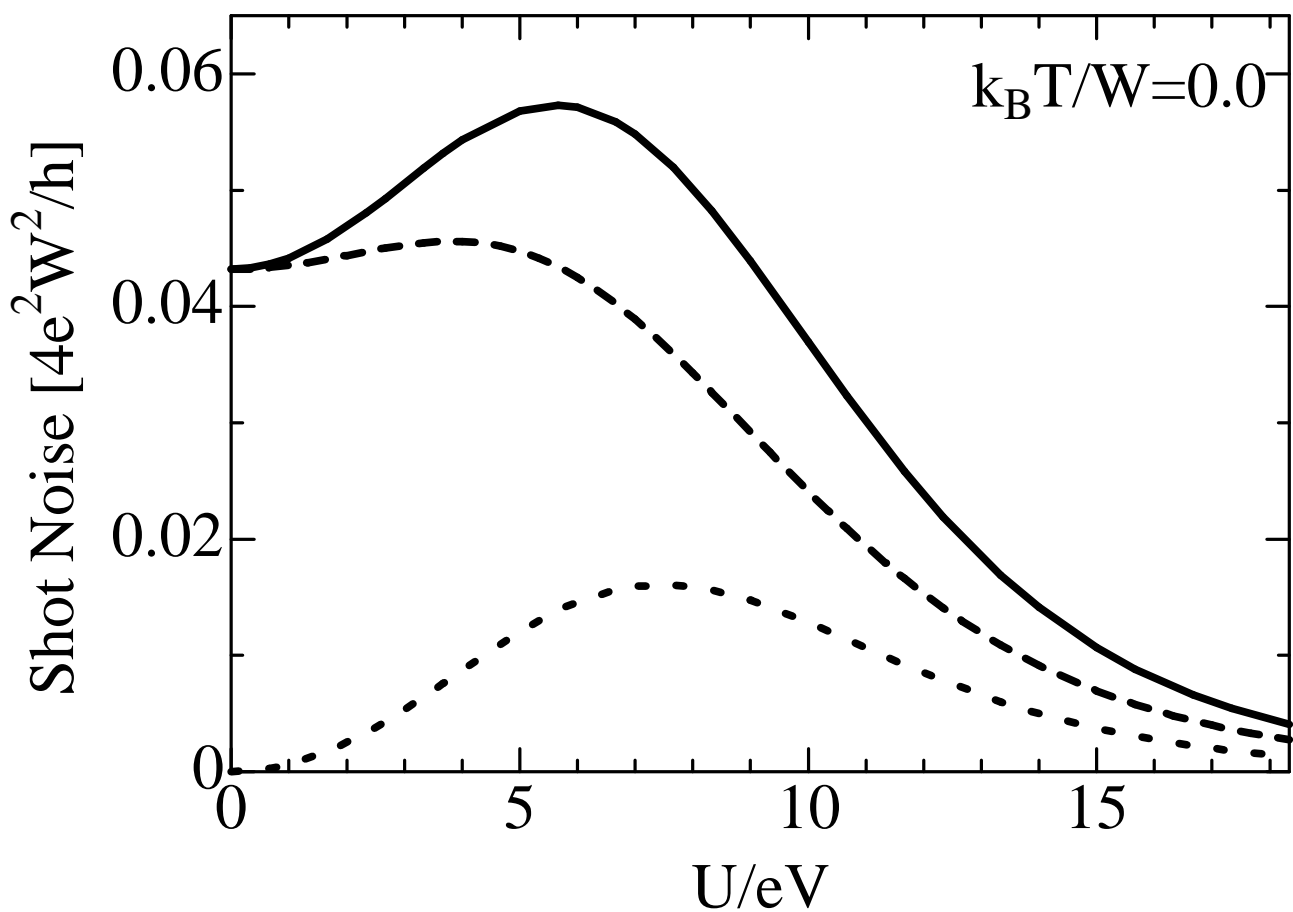


Fig.7(a)      Hamasaki

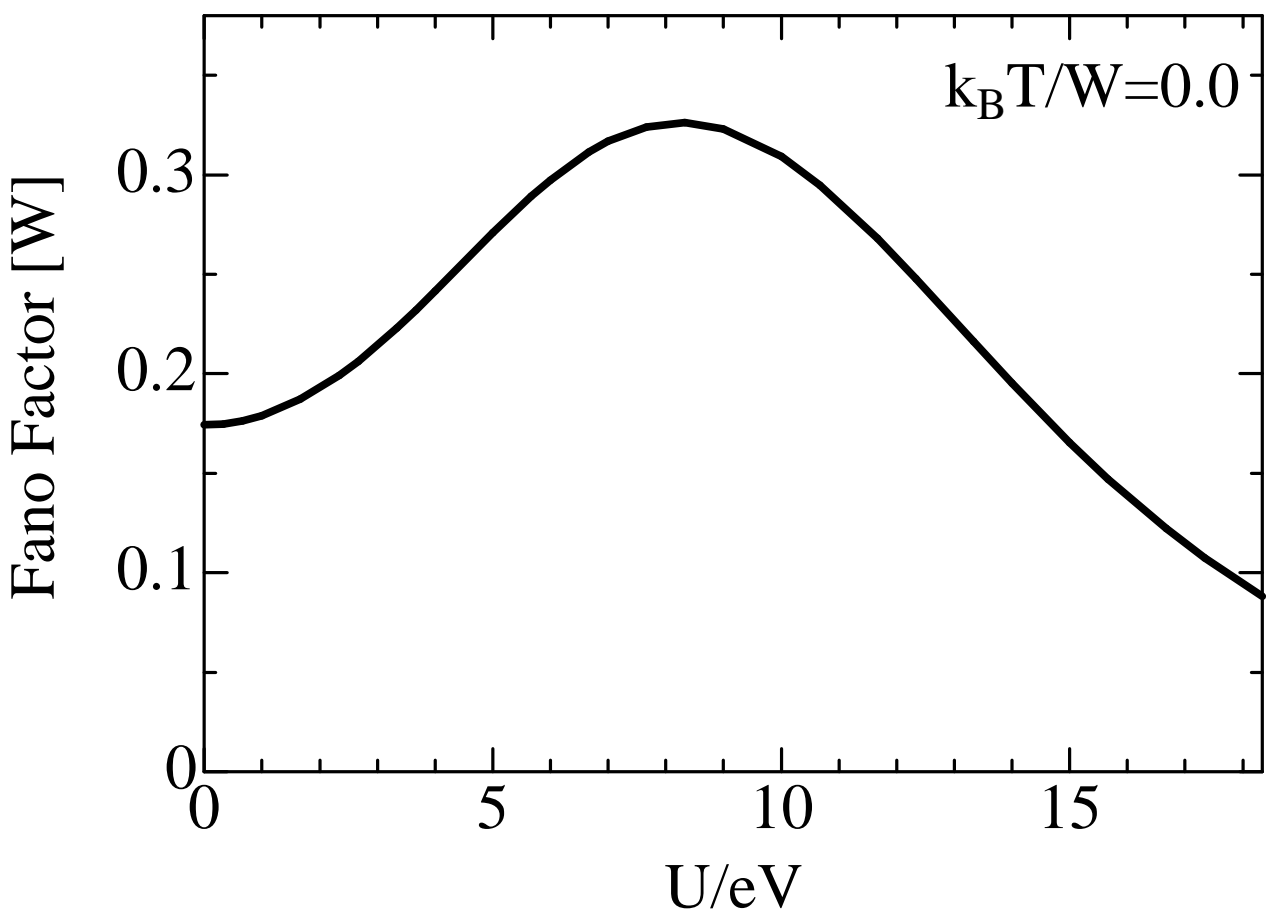


Fig.7(b)    Hamasaki

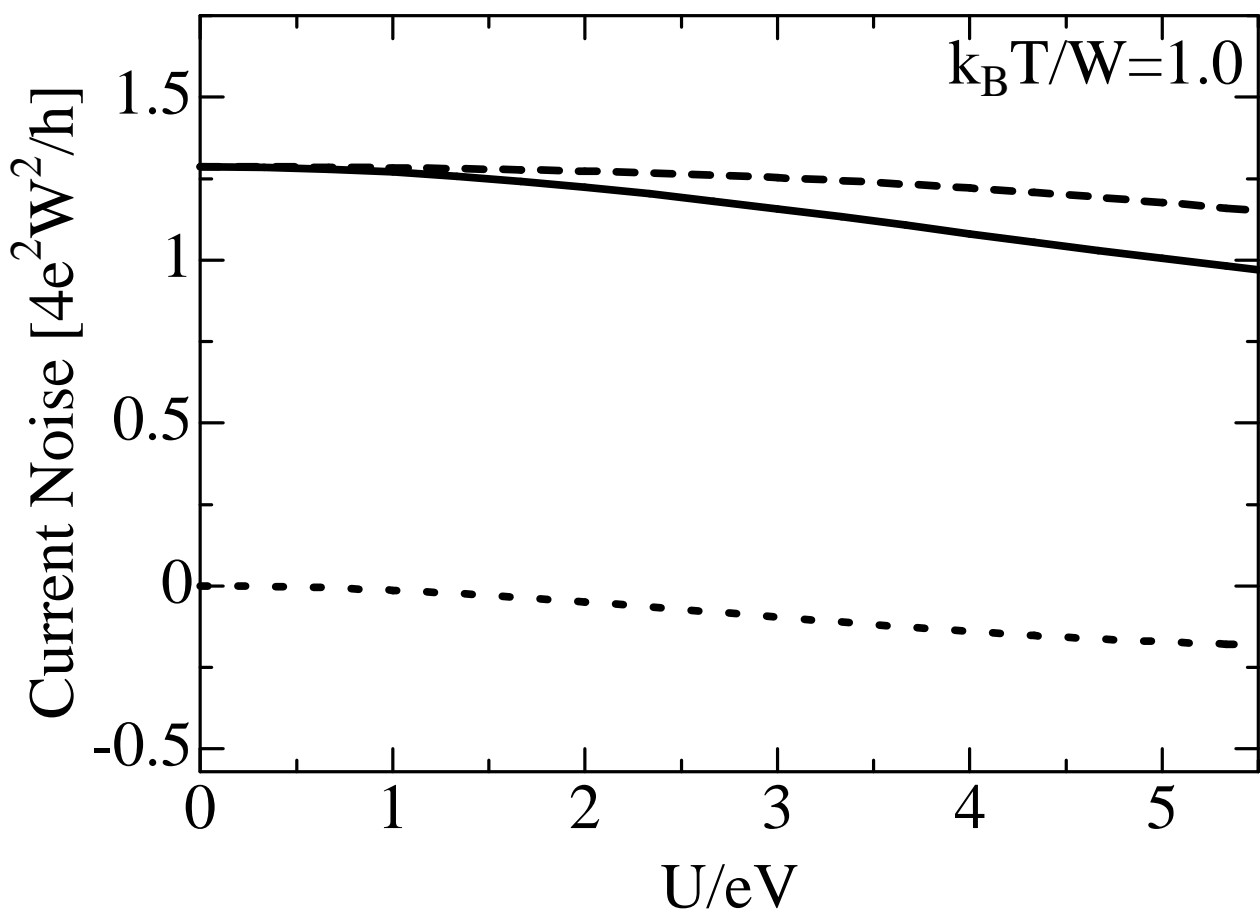


Fig.8 Hamasaki